Contract No.:

This manuscript has been authored by Savannah River Nuclear Solutions (SRNS), LLC under Contract No. DE-AC09-08SR22470 with the U.S. Department of Energy (DOE) Office of Environmental Management (EM).

In-situ and *ex-situ* comparison of the electrochemical oxidation of SO_2 on carbon supported Pt and Au catalysts.

Authors

Benjamin H. Meekins[1]	ben.meekins@gmail.com
Anthony B. Thompson[2]	anthony.thompson@srnl.doe.gov
Varsha Gopal[1]	vgopal@email.sc.edu
Bahareh A. Tavakoli Mehrabadi[3]	btavakol@andrew.cmu.edu
Mark C. Elvington[4]	mark.elvington@src.energy
Prabhu Ganesan[4]	prabhu.ganesan@src.energy
Ty A. Newhouse-Illige[5]	tnewhouse@pvdproducts.com
Adam W. Shepard[5]	ashepard@pvdproducts.com
Lawrence E. Scipioni[5]	lscipioni@pvdproducts.com
James A. Greer[5]	jgreer@pvdproducts.com
John C. Weiss[1]	jcweiss@email.sc.edu
John W. Weidner[1]	weidner@engr.sc.edu
Héctor R. Colón-Mercado*[,2]	hector.colon-mercado@srnl.doe.gov

Affiliations

[1] Department of Chemical Engineering
The University of South Carolina,
Columbia, South Carolina, 29208, USA

[2] Integrated Energy Systems
Savannah River National Laboratory
Aiken, South Carolina, 29808, USA

[3] Department of Mechanical Engineering
Carnegie Mellon University
Pittsburgh, PA 15213, USA

[4] Savannah River Consulting, LLC
301 Gateway Drive
Aiken, South Carolina 29803, USA

[5] PVD Products, Inc.
35 Upton Drive, Suite 200
Wilmington, MA, 01887, USA

* Corresponding author

Highlights

- Au is more active and stable than Pt, Pd, and Ir for electro-oxidation of SO_2
- Electrolyzer experimental results confirm *ex-situ* electrochemical observations
- Au provides a pathway to new catalysts that can meet projected performance targets

Abstract

Electrochemical characterizations are performed using thin films and commercial carbon supported platinum and gold catalysts for sulfur dioxide oxidation, the primary electrochemical oxidation reaction in the Hybrid-sulfur (HyS) thermochemical process. Electrochemical evaluation of metal thin films qualitatively confirms the higher activity of Au over Pt, AuPt, Pd, and Ir for the electrochemical oxidation of SO_2. *Ex-situ* testing using rotating disk electrode (RDE) shows an earlier onset potential for Au/C at low sulfuric acid concentrations ($C \leq 3.5$ M) and a higher turnover frequency than Pt/C at sulfuric acid concentrations ranging from 3.5 M to 9 M. *In-situ* electrolysis experiments using low catalyst loadings (0.1 mg_{Au} cm^{-2}, a factor of ≥ 5 lower than typical loadings) confirm that Au nanoparticles exhibit higher current densities and greater stability than Pt nanoparticles. This is consistent with the thin film screening studies, which showed higher activity with increasing gold content in AuPt thin films. This work provides an alternative material to state-of-the-art Pt to lower the energy needs and aid the HyS cycle in reaching the target of \$2/kg H_2 set forth by the Department of Energy to achieve economic feasibility of large-scale hydrogen generation.

Keywords

Hybrid Sulfur, gold catalyst, platinum catalyst, hydrogen production, sulfur dioxide electrochemical oxidation

1.0 Introduction

Efficient and clean energy conversion technologies are required in order to satiate the energy needs of modern society while reducing the environmental impact of carbon-based energy technologies. Hydrogen is an attractive alternative, as an energy carrier and as a feedstock to chemical industries such as ammonia production and petroleum refining[1]. However, current large-scale hydrogen production methods generally rely on steam reforming, an energy intensive and environmentally unfavorable process[2]. To the present-day, the preferred method for producing clean hydrogen is water electrolysis, which is also energy intensive and an expensive enterprise, mostly due to kinetic limitations. The hybrid sulfur (HyS) process, an electrochemical/thermochemical hybrid cycle, offers an alternative for large scale hydrogen production. When coupled with carbon-free high-temperature heat and electricity, the hybrid sulfur cycle is capable of producing inexpensive carbon-free hydrogen in large quantities[3, 4].

The HyS cycle consists of a low and a high temperature step. In the low temperature step, sulfur dioxide (SO_2) is electrochemically oxidized with water to produce hydrogen (H_2) and sulfuric acid (H_2SO_4). While the electrochemical oxidation reaction occurs at a thermodynamic potential of $E° = -0.157$ V vs SHE[5], practical currents are not observed until overpotentials greater than 300 mV are applied at 80 °C. Even with the high overpotential, this represents a facile reaction compared to oxidation of water ($E^o = -1.23$ V vs SHE), which also typically requires large overpotentials of at least 200 mV. Except for a few research groups, the focus on the electrochemical oxidation of sulfur dioxide has centered on the electrolyzer performance using platinum based electrocatalysts[6-13]. Xue[12] *et al*. investigated the role of transition metals present in Pt based alloy electrocatalysts in an electrolysis cell. They reported moderate improvements both in the open circuit potential and high currents in the high current density region of the electrolysis with the use of $PtCr_2/C$. On the other hand, O'Brien[14] and Quijada[15]

have studied the electrochemical oxidation of SO_2 using Au and Pt polished disk electrodes. Their work showed that both bulk Pt and Au are active catalysts for the SO_2 oxidation reaction. In fact, Au appeared to exhibit far better overall performance for SO_2 oxidation than Pt. The improved performance of Au could be explained by noting that the Au surface remains relatively free of strongly adsorbed SO_2, which allows substantial catalytic activity for SO_2 oxidation on unmodified electrodes[16]. However, after careful modification of the Pt surface with adsorbed sulfur, the electrocatalytic activity of Pt can be made comparable to that of Au[17]. In a similar work, Zelinsky[18] studied the effect of surface activation of gold surface on the SO_2 oxidation . His work showed that after a "sulfur adlayer" is formed, the maximum current peak shifts 200 mV to lower potentials indicating the activation of the catalyst surface. The improvement in Pt electrochemical activity through surface activation seems to be attributed to a shift in the onset potential for SO_2 oxidation to values below Au[14]. The slope of the mixed kinetic-diffusion limited region for Au, however, remains higher than that of Pt. Modeling results for SO_2 electrooxidation on single plane transition metals support the experimental observations, which show the SO_2 oxidation rate is higher in Au, followed by Pt, Pd, Ag, and Ir[19]. There are inconsistent results, however, reported in the literature due to the complex behavior of sulfur species on metal surfaces. Falch *et al.*[20] evaluated the activity of Pt, Pd, Au, and PtPd alloy thin films and reported the activity based on the onset potential. They reported that PtPd bimetallic alloys was more active than pure Pt, and in the case of pure metals, the best activity was obtained in the order Pt > Pd > Au. Despite the promising high electrochemical activity from bulk and thin films observed for various metals, there is a dearth of experimental research on nanoparticles supported on carbon that are used in an electrolysis cell[13]. It is possible that the electrochemical properties observed for the metal as nanoparticles to be significantly different

compared to its bulk metal properties, as was observed in our earlier experimental work[21]. Bulk Pd was previously identified to have SO_2 electrooxidation performance on par with Pt[22], but when tested as a supported nanoparticle on carbon black, the performance of Pd was much lower than Pt, and also did not show adequate electro-chemical stability[21]. It is important to note that carbon black does not impart catalytic activity to the supported metal nanoparticles[21, 23] and only acts as an electrical conductor and anchoring support for the metal nanoparticles. In the present work, we performed screening studies to evaluate the electrochemical activity of Pt, Au, Ir, and Pd thin films. Furthermore, because of the low onset potential of Pt, as well as the large kinetic current slope observed for Au, the effect of bimetallic alloys between Pt and Au was elucidated by high-throughput thin film electrochemistry using SECM. Finally, we evaluated and compared the electrocatalytic performance of commercial Au/C and Pt/C for the SO_2 oxidation reaction in two systems, a rotating disk electrode and a gas fed sulfur dioxide depolarized electrolyzer (SDE).

2.0 Materials and methods

2.1 Materials: Physical vapor deposition targets were obtained from Alfa Aesar and Kurt J. Lesker Company with a purity of > 99.9%. Mirror polished Sigradur® glassy carbon plates were obtained from (HTW Hochtemperatur-Werkstoffe GmbH). 20 wt% Au on Vulcan XC-72 (Premetek), 40 wt% Pt on Vulcan XC-72 (BASF), ethanol (200 proof, Sigma-Aldrich), methanol (for HPLC, Sigma Aldrich), Nafion® ionomer (D-520, Alfa Aesar), sodium sulfite anhydrous (low phosphate, Fisher Scientific), sulfur dioxide (anhydrous, Matheson), carbon paper (Sigracet 29 BC, FuelCellStore), Nafion® membrane (Nafion® 115, FuelCellStore), and sulfuric acid (ACS reagent, Sigma-Aldrich) were all used as received.

2.2 Thin Film Electrochemical Screening: Thin film deposition was performed by magnetron sputtering ~200 nm films of Pt, Au, Ir, and Pd on mirror polished glassy carbon coupons. The

deposition was carried out by applying 60 W of power in an Ar atmosphere at 0.467 Pa. Once coated, the coupons were mounted on a flat specimen corrosion cell purchased from AMETEK which exposes 1 cm^2 area of the coupon to the test solution. The thin films were evaluated in 3.5 M sulfuric acid saturated with SO_2. The three-electrode cell consisted of a graphite rod counter electrode and a double junction Ag/AgCl reference electrode. After the solution was saturated with SO_2, the electrochemical activity was evaluated by scanning from 0.9 V to 0.3 V vs NHE at 50 mV/s. The electrochemical performance was reported after surface activation.

High-throughput screening was carried out on a scanning electrochemical microscope (SECM; Princeton Applied Research/Uniscan Instruments) using a glassy carbon substrate with thin films containing of various Au and Pt ratios (Figure 1A**).** Samples were prepared by magnetron sputter co-deposition of Au and Pt. Composition was controlled by varying the power to each target. Electrochemical measurements were conducted using a scanning droplet system (SDS; Bio-Logic Science Instruments) cell attachment on the SECM (Figure 1B). A three-electrode electrochemical cell consisting of a silver/silver sulfate (Ag/Ag_2SO_4) reference electrode (Koslow Scientific Co.) and a Pt wire counter electrode was used for the screening studies. The Ag/Ag_2SO_4 reference electrode potential was calibrated by using Ag/AgCl as well as NHE reference electrodes. A solution of 0.1 M sodium sulfite (Na_2SO_3) in 0.1 M H_2SO_4 was used as an SO_2 precursor. Cyclic voltammetry experiments were conducted from -0.20 to 0.60 V vs. Ag/Ag_2SO_4 (0.28 to 1.08 V vs. NHE) at a scan rate of 150 mV/s.

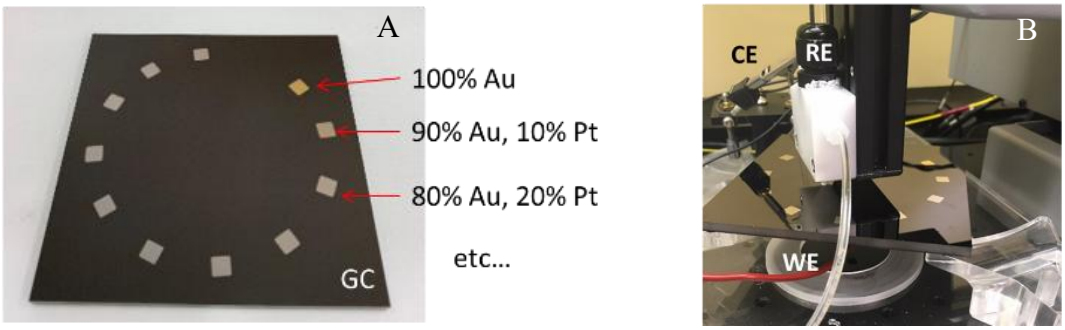

Figure 1. (A) Combinatorial thin film catalysts on glassy carbon substrate; (B) scanning droplet system cell for scanning electrochemical microscope.

2.3 Rotating Disk Electrode: Rotating disk electrode experiments were conducted using a polished glassy carbon electrode (5 mm diameter, Pine Instruments) in 50 mM Na_2SO_3 dissolved in H_2SO_4 at concentrations of 3.5 M, 7 M, and 9 M. All catalyst inks were prepared by mixing the catalyst (1.7 mg of metal) with 4.2 mL of deionized water, 1.7 mL of ethanol, and 22 µL of Nafion® ionomer, such that the metal catalyst was held constant at 0.287 mg mL^{-1}. After the ink was sonicated for 1 hour in an ice bath, 18.5 µL of catalyst ink was pipetted onto the glassy carbon electrode and allowed to dry at room temperature. A constant metal loading of 27.5 μg_{Metal} cm^{-2} on the RDE tip was used for all experiments. The counter electrode consisted of a coiled Pt wire. The reference electrode consisted of a double junction Ag/AgCl reference electrode. Prior to all measurements, the reference potential was measured in a 0.1 M H_2SO_4 solution against a Pt wire bubbled with H_2. All potentials reported herein have been converted to the NHE. Hydrodynamic curves were obtained by cycling the RDE at 50 mV sec^{-1} from 0.3 V to 1.2 V vs. NHE. Rotations were performed from 400 to 1600 RPM at 200 RPM intervals. Anodic scans at 400 RPM were reported after one complete cycle.

2.4 Electrolyzer: Membrane electrode assemblies (MEAs) were prepared by direct spraying of the catalyst ink onto the membrane. The ink was prepared by mixing 400 mg of catalyst with 1.5

g of deionized water, followed by 24 g of methanol. After ultrasonically mixing for 5 minutes, 1.4 g of Nafion® ionomer was added. The ink was then sonicated in an ice bath for one hour. Afterwards, the ink was loaded to an automated ultrasonic sprayer (Prism-400BT, Ultrasonic Systems, Inc.), where it was mixed for an additional 30 minutes. The membrane was placed on a vacuum heated plate (at 80 ºC) where a coating area of 25 cm^2 with the desired loading was reached on each side. The cathode catalyst loading was maintained at 0.3 mg_{Pt} cm^{-2}, while the anode catalyst loading was maintained at 0.1 mg_{Metal} cm^{-2}. The MEA was assembled in a 25 cm^2 single serpentine redox flow cell (Scribner) by placing 254 μm thick PTFE gasket followed by the carbon paper, the MEA, carbon paper, and another 254 μm thick PTFE gasket. Once assembled, the bolts where tightened with a torque of 14 N-m. The cell fixture was connected to a custom test station. In a typical test, the cell is purged with N_2 while the cell and the delivery lines heat to 90 ºC. Once at temperature, a voltage of 0.95 V is applied using a high current potentiostat (HCP-803, Biologic) followed by a flow of 1.7 mL min^{-1} H_2O at the cathode and ~165 sccm of SO_2 plus 3 mL min^{-1} of H_2O at the anode (water stoichiometry of 8.3). Once steady state currents are observed, a cathodic scan is measured from 0.95 V to 0.65 V at a rate of 0.1 mV/s. Additionally, the high frequency resistance was measured every 50 mV using galvanostatic electrochemical impedance spectroscopy. A perturbation current of 100 mA was used for this experiment.

2.5 Electron microscopy and particle size distribution: Transmission electron microscopy (TEM) images were collected on a Hitachi HT7800 with an accelerating voltage of 100 kV and lattice resolution of 0.2 nm. Samples were deposited on lacey carbon grids. Particle sizes were determined using ImageJ and a known pixel-to-nm ratio. A minimum of 35 measurements were

made across multiple images for both Au and Pt nanoparticles on carbon support to ensure a representative sample was collected.

3.0 Results and Discussion

Surface activation can have a large influence on the electrochemical activity of metals for the SO_2 oxidation reaction. Because of the complex processes occurring at the catalyst surface, interpretation of the results can be problematic. We believe that the testing protocol employed on the catalyst screening eliminates many of the inconsistencies associated with the values reported in the literature. The screening of the different metal substrates was performed in the potential range between 0.3 V and 0.9 V vs NHE. This potential range limits undesirable surface reactions associated with excessive sulfur deposition at low potentials and catalyst surface oxidation at high potentials[24], while monitoring the surface activation. Figure 2A shows a typical linear sweep voltammetry plot for the Pt thin film. As observed in the figure, the activity of Pt improves with cycling and the performance stabilizes after 8 cycles. The onset potential for SO_2 oxidation obtained for the various thin films is plotted in Figure 2B. As observed in the figure, most metals undergo a surface activation. For Au, activation occurs quickly, however the performance starts to degrade after the fourth cycle. This kind of degradation may be caused by the accumulation of sulfur species on the surface, especially those generated at the low potentials of the counter electrode which can migrate and poison the working electrode. In contrast, Pd thin films did not show a surface activation. This behavior can be ascribed to the unstable nature of Pd under the testing conditions[21]. For consistency purposes, the activity of the various films is evaluated at a cycle number where the best performance is observed and the results are shown in Figure 2C. As expected, the best performance is obtained for Au and Pt thin films followed by Pd and finally Ir. It is surprising that the onset potential is almost identical for the Au and Pt thin films. However, the performance of Au at high current densities is more than an order of

magnitude higher than that of Pt.

Among the metals tested in the screening study, it can be concluded that Pt and Au thin films exhibit superior performance for the electrochemical oxidation of sulfur dioxide. While Au thin films show quick activation and high current densities at lower potentials; it also shows some catalyst deactivation as the material is cycled. On the other hand, Pt thin films take longer duration for activation. However, after the surface is activated, stable performance is observed in the potential range tested. Ideally, a material that combines the positive attributes of Pt and Au should result in a superior catalyst for SO_2 oxidation. For this purpose, thin films of Pt with various amounts of gold were prepared and evaluated in SECM.

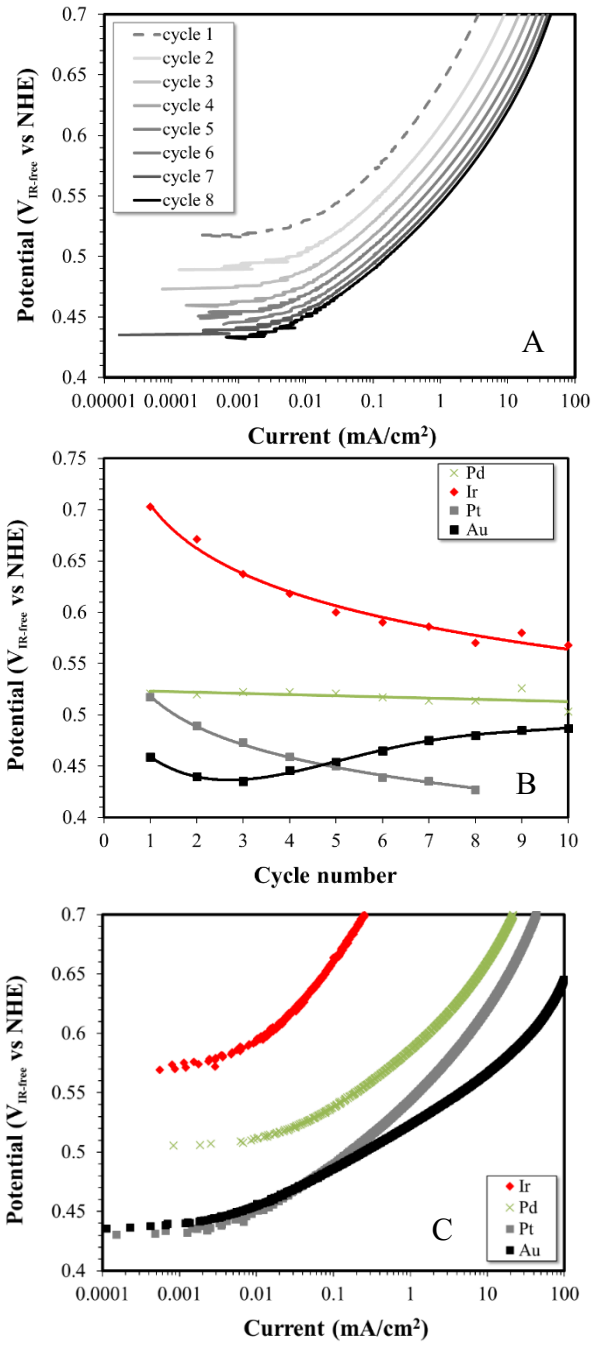

Figure 2. (A) Linear sweep scans for the electrolysis of SO_2 on thin films in 3.5M sulfuric acid saturated with sulfur dioxide measured at 50 mV/s, (B) Cycle life studies of various thin film catalysts, and (C) Comparison of best polarization performance selected from cycle life studies for various thin film catalysts

Figure 3 shows the SECM results of activity of combinatorial thin films for the electrochemical SO_2 oxidation as a function of Au and Pt content at two different applied potentials. A low (0.58 V) and high (1.08 V) potential were selected in order to probe the

reaction kinetics closer to the onset potential (activation region) and at the kinetically limited region, respectively. In the activation region, a weak correlation is observed between gold content and catalytic activity. This correlation can be expected as similar onset potentials between Pt and Au were observed in Figure 2C. However, a clearer trend emerges in the kinetically limited region, with activity increasing significantly with an increase in gold concentration. Although differing experimental conditions do not allow quantitative comparison with linear sweep voltammetry, the SECM results qualitatively confirm the higher activity of gold over platinum for the electrochemical oxidation of SO_2.

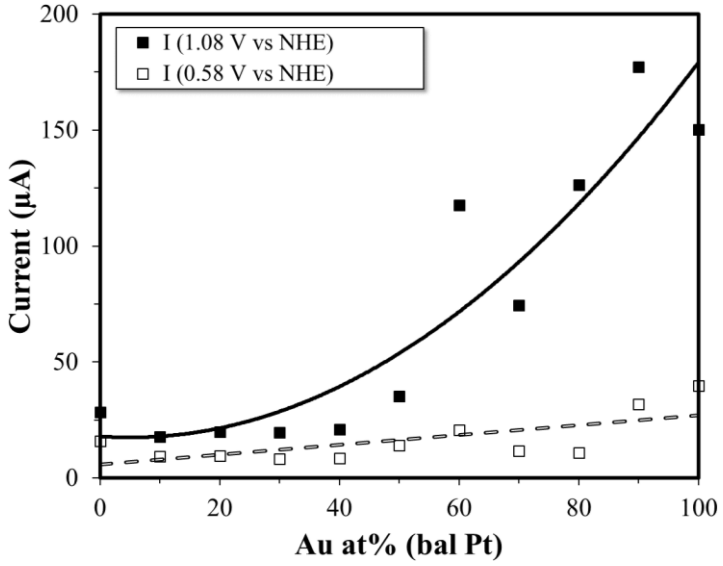

Figure 3. Electrochemical activity (current) obtained from AuPt thin film samples at two applied potentials as a function of composition.

Au/C catalysts with a similar particle size to the Pt/C catalysts were selected to minimize any possible particle size effect on the electrochemical performance. TEM images of the 20 wt% Au/C and 40 wt% Pt/C commercial catalysts show well distributed nanoparticles on their respective carbon support, Figure 4. An analysis of the particle size distribution for the different electrocatalysts shows a unimodal size distribution. The Au/C and Pt/C nanoparticles had an average diameter of 2.3 ±0.6 nm and 3.4 ±0.9 nm, respectively (see Figure 5). It is important to

mention that the same metal loading was used for all the electrochemical measurements because the metal weight percentages of Pt/C (40 wt%) and Au/C (20 wt%) are different.

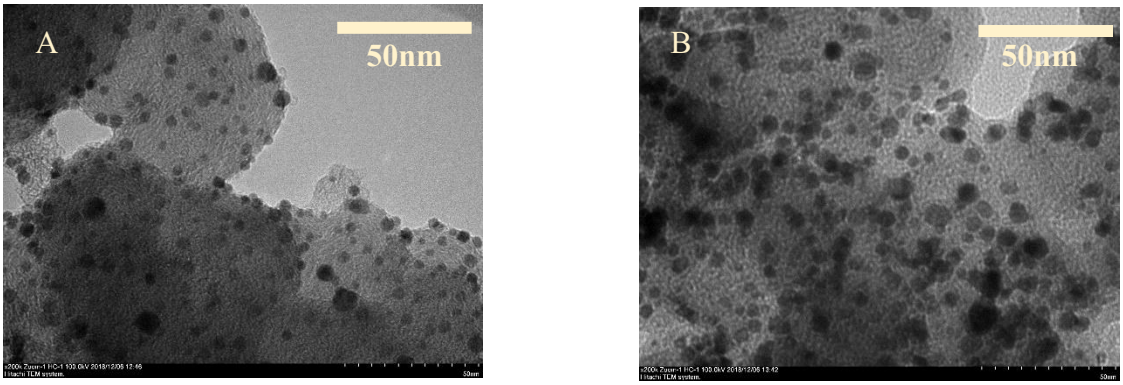

Figure 4. TEM images of 20% Au/C (A) and 40% Pt/C (B).

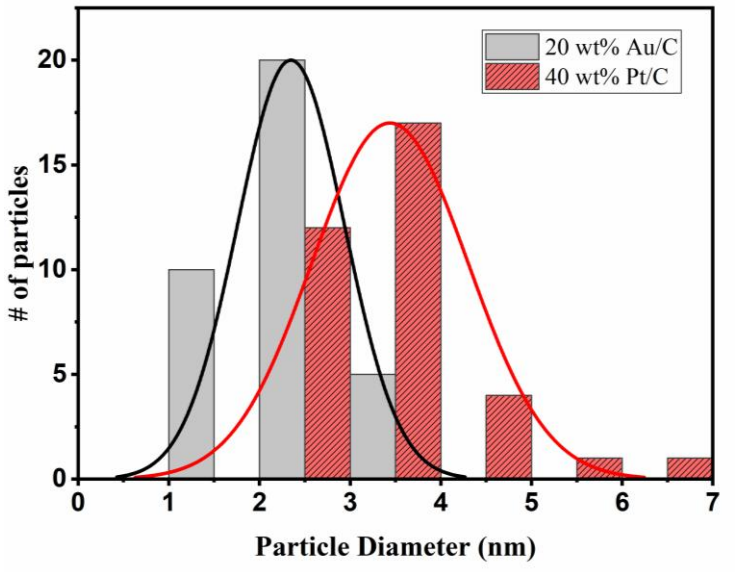

Figure 5. Size distribution of Au/C and Pt/C commercial catalysts with normal Gaussian fits.

Prior literature reports have shown that acid electrolyte concentration can impact the catalysts' electrochemical activity by varying diffusion limitations[14]. This observation was taken under consideration while evaluating the electrocatalysts via rotating disk electrode (RDE). Various concentrations of sulfuric acid solutions with 50mM sodium sulfite salt (Na_2SO_3) were used as well-defined surrogates instead of dissolved SO_2. It is important to note that during *in-*

situ electrolyzer testing, it is difficult to predict the local acid concentration at the electrode layer due to possible mass transport limitations. Therefore, understanding the effect of sulfuric acid concentration on RDE performance can help predicting the environment at the catalyst layer in the electrolyzer. Once a thin layer of catalyst powder was loaded onto the RDE tip, we conducted sulfite oxidation in increasingly concentrated sulfuric acid solutions with a rotation speed of 400 RPM (Figure 6). The first noteworthy observation is that there is a significant difference in the limiting current that is dependent on the acid concentration. Although the sodium sulfite concentration is constant in all acid solutions, a continuous decrease in limiting currents is observed as the acid concentration increases which is in agreement with the published literature results for polished disk electrode experiments[14]. This effect is attributed to changes in the diffusion coefficient and kinematic viscosity. In the 3.5 M sulfuric acid solution, Au has a lower onset potential for the oxidation of sulfite to sulfate. The diffusion-limited currents observed for Au and Pt catalyst are similar. In 7 M sulfuric acid, Pt has a lower onset potential, but Au has a higher limiting current and outperforms Pt from about 0.57 V to approximately 1.1 V (vs. NHE). In 9 M sulfuric acid, Pt again has a slightly lower onset potential, but Au again exhibits higher limiting current and outperforms Pt from about 0.62 V until 1.0 V. Au has just one oxidation peak under all acid concentrations tested. Pt, however, has a second oxidation step that is observed in both 7 M and 9 M H_2SO_4 concentrations at approximately 0.95V. It is possible that the second oxidation step is influenced by the formation of a Pt oxide layer[25].

Kinetic currents were then derived at each potential at a rotation speed of 400 RPM using the following relationship[26] $i_k = i_d\, i/(i_d - i)$, where i_k is the kinetically limited current, i_d is the diffusion limited current and i is the total disk current. Several trends can be observed from Figure 6. First, higher acid concentrations reduce the kinetic currents for both Au and Pt;

however, the effect of acid concentration is more significant on gold. Au has higher kinetic currents than Pt beginning at 0.42 V for 3.5 M, 0.57 V for 7 M, and 0.62 V for 9 M, which is profoundly significant considering the operational target for the SO_2 depolarized electrolyzer (SDE) is 0.6 V. This data indicates that the Au catalyst is a promising candidate for the SDE.

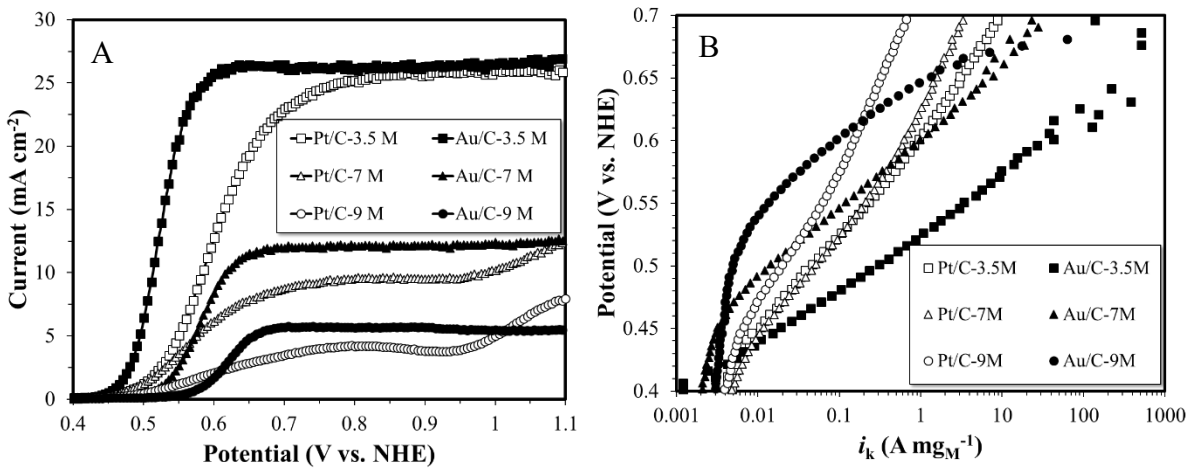

Figure 6. A) Linear sweep voltammetry of 20% Au/C (solid symbols) and 40% Pt/C (open symbols) in 3.5M (squares), 7M (triangles), and 9M (circles) sulfuric acid, all with 50 mM sulfite measured at 50 mV/s and B) kinetic currents. Note: Noise observed at high potentials is due to approaching the diffusion-limited current.

The electrochemical performance of Pt/C and Au/C catalysts were also evaluated in an electrolysis cell. Note that while published literature has identified Au as a possible candidate for the SDE, there are no published studies that evaluate Au/C in an actual electrolysis cell. In the present experiments, the metal loading on the anode remained the same for both Pt/C and Au/C, but lower loadings (0.1 mg_M cm^{-2}) than typically published in the literature (~1 mg_M cm^{-2}) [9, 11] were used. The lower loadings were selected to facilitate evaluations of the kinetically limited regions of the electrolyzer performance. As observed in Figure 7A, the SO_2 electrooxidation performance of the Au/C catalyst is superior to that of the Pt/C catalyst, confirming the RDE results. In addition, the high frequency resistance (HFR) is very similar for cells employing Pt/C and Au/C, indicating that the difference in performance is entirely due to the catalyst. The HFR increase as a function of current can be correlated to a local increase in

acid concentration at the catalyst/membrane interface. The electrolyzer was not operated at potentials lower than 0.6 V to limit unreacted sulfur dioxide crossover to the cathode[11, 27]. Plotting the IR-free potential vs. normalized cell current, Figure 7B, facilitates the comparison of catalyst performance in both RDE and electrolyzer. The current values of Pt/C and Au/C catalysts obtained at various operating potentials are summarized in Table 1. The currents measured for Pt and Au in the electrolyzer operated at 90 ºC are on the same order of magnitude as the currents measured for the RDE at 9 M. This seems to indicate that the local acid concentration in the electrolyzer is close to 9 M. This result is expected as the local concentration in sulfuric acid can increase very quickly if the acid product is not removed as it is formed. The fact that the IR corrected electrolyzer performance shows a large slope could indicate that the electrode in the electrolyzer suffers from mass transport limitations. Future studies on electrode design will need to be performed to lower the mass transport limitations. One important note is that we observe 1 A mg_{Au}^{-1} at 0.6 $V_{IR\text{-}free}$, which indicates that, with improvements in the electrode fabrication techniques and an increase in loading from 0.1 $mg_{Au}\,cm^{-2}$ to more conservative loadings of 0.5 $mg_{Au}\,cm^{-2}$, the electrolyzer could become close to meeting the performance target set by techno-economic analysis studies[3].

The short-term stability of the catalyst was also evaluated at various potentials and the results are summarized in Table 2. These results clearly indicate that while both Au and Pt retain catalytic activity at potentials ≥ 0.85V, below that potential Pt exhibits a precipitous decline in performance. In comparison, Au retains its activity over the same timeframe. Anode catalyst stability at lower potentials is vital for meeting the ultimate performance goal of 0.5 A cm^{-2} at an operating potential of 0.6V. The stable performance of Au corroborates our hypothesis that the performance degradation observed in Figure 2B was caused by the accumulation of sulfur

species generated at the low potentials on the counter electrode which then migrated to the Au electrode.

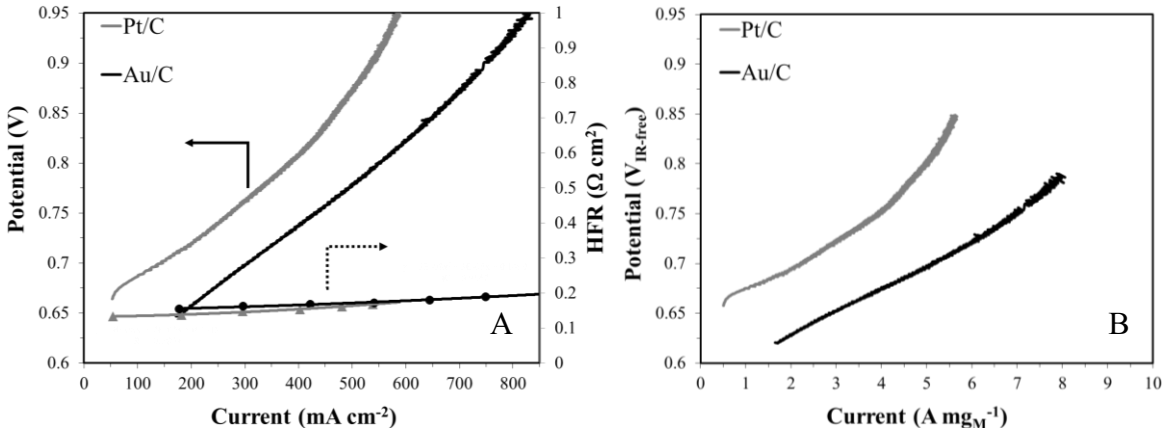

Figure 7. A) Sulfur dioxide performance curve for anodes with Pt/C (grey trace) and Au/C (black trace). B) IR free potential vs. normalized cell current. Anode metal loading is 0.1 mg cm^{-2} for all cases.

Table 1. Comparison of kinetic currents from rotating disk electrode and electrolyzer.

Potential (V)	**SDE @ 90 ºC (A mg_{Metal}^{-1})**		**RDE @ 20 ºC (A mg_{Metal}^{-1})**					
			3.5 M		7 M		9 M	
	Pt/C	Au/C	Pt/C	Au/C	Pt/C	Au/C	Pt/C	Au/C
0.65	$5.0x10^{-1}$	2.9	3.0	$5.0x10^{2}$	1.6	7.8	$3.3x10^{-1}$	1.3

Table 2. Electrolyzer performance for Pt/C and Au/C over time at various operating potentials. Performance measured at 90 ℃ after 5 minutes and 60 minutes of potential hold.

Potential (V)	**Pt/C (mA cm^{-2})**		**Au/C (mA cm^{-2})**	
	After 5 min	After 60 min	After 5 min	After 60 min
0.95	558	553	818	843
0.85	421	429	674	674
0.75	237	74	428	410

4.0 Conclusions

We have shown in this work that Au is not only a possible substitute for Pt for catalyzing electrooxidation of SO_2 to H_2SO_4 but is actually a more active and stable catalyst than Pt, Pd, and Ir. Screening studies on PtAu thin films showed a monotonic increase in activity as Au concentration increases. For all acid concentrations employed in the present study, Au/C

exhibits higher limiting currents in RDE experiments than Pt/C, indicating higher turnover frequency. Further, when used in an actual electrolysis cell, Au/C allows for lower potentials to achieve the same current density as Pt/C with similar loadings. We also note that with an increase in loading from 0.1 mg cm^{-2} to 0.5 mg_{Au} cm^{-2}, the IR-free polarization curve shows that 0.5 A cm^{-2} at 0.6 V is achievable. Importantly, this work was performed using a Nafion® membrane, which exhibits an exponential increase in resistance with increases in acid concentration and is limited to temperatures ≤ 100 ^{o}C. We have demonstrated previously[6] that sulfonated polybenzimidazole (s-PBI) membranes have acid concentration-independent resistance (~0.05 Ω cm^2) and can be operated at temperatures up to 160 ^{o}C, pushing the cell potential needed for 0.5 A cm^{-2} to 0.66V using a Pt/C catalyst. We anticipate that utilizing a Au/C catalyst, as shown in this work, along with s-PBI membrane will facilitate an even greater reduction in cell voltage. Finally, this work provides an alternative material to state-of-the-art Pt to lower the energy required to drive the HyS cycle and aid in reaching the target of \$2/kg H_2 set forth by the Department of Energy in order to achieve economic feasibility of large-scale hydrogen generation while reducing the cost of expensive noble metal catalysts.

5.0 Acknowledgements

Financial support was provided by Savannah River National Laboratory's Laboratory Directed Research and Development program. Savannah River National Laboratory is managed and operated by Savannah River Nuclear Solutions, LLC under Contract No. DE-AC09-08SR22470 with the United States Government.

Graphical Abstract

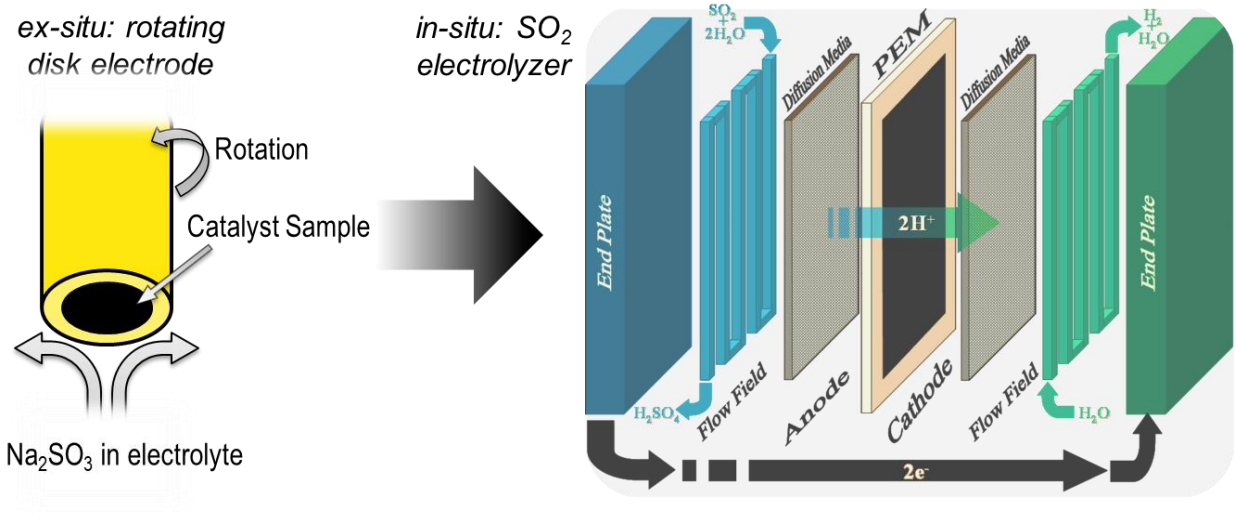

References

1. Pivovar, B.; Rustagi, N.; Satyapal, S., Hydrogen at Scale (H2@ Scale): Key to a Clean, Economic, and Sustainable Energy System. *Electrochem. Soc. Interface,* **2018,** *27*, 47-52.
2. Jarvis, S. M.; Samsatli, S., Technologies and infrastructures underpinning future CO2 value chains: A comprehensive review and comparative analysis. *Renewable and Sustainable Energy Reviews,* **2018,** *85*, 46-68.
3. Gorensek, M. B., Hybrid sulfur cycle flowsheets for hydrogen production using high-temperature gas-cooled reactors. *Int. J. Hydrogen Energy,* **2011,** *36*, 12725-12741.
4. Gorensek, M. B.; Corgnale, C.; Summers, W. A., Development of the hybrid sulfur cycle for use with concentrated solar heat. I. Conceptual design. *Int. J. Hydrogen Energy,* **2017,** *42*, 20939-20954.
5. Gorensek, M. B.; Staser, J. A.; Stanford, T. G.; Weidner, J. W., A thermodynamic analysis of the SO2/H2SO4 system in SO2-depolarized electrolysis. *Int. J. Hydrogen Energy,* **2009,** *34*, 6089-6095.
6. Garrick, T. R.; Wilkins, C. H.; Pingitore, A. T.; Mehlhoff, J.; Gulledge, A.; Benicewicz, B. C.; Weidner, J. W., Characterizing Voltage Losses in an SO2 Depolarized Electrolyzer Using Sulfonated Polybenzimidazole Membranes. *J. Electrochem. Soc.,* **2017,** *164*, F1591-F1595.
7. Jayakumar, J. V.; Gulledge, A.; Staser, J. A.; Kim, C. H.; Benicewicz, B. C.; Weidner, J. W., Polybenzimidazole Membranes for Hydrogen and Sulfuric Acid Production in the Hybrid Sulfur Electrolyzer. *ECS Electrochem. Lett.,* **2012,** *1*, F44-F48.
8. Staser, J. A.; Norman, K.; Fujimoto, C. H.; Hickner, M. A.; Weidner, J. W., Transport Properties and Performance of Polymer Electrolyte Membranes for the Hybrid Sulfur Electrolyzer. *J. Electrochem. Soc.,* **2009,** *156*, B842-B847.
9. Staser, J. A.; Gorensek, M. B.; Weidner, J. W., Quantifying Individual Potential Contributions of the Hybrid Sulfur Electrolyzer. *J. Electrochem. Soc.,* **2010,** *157*, B952-B958.

10. Hobbs, D. T.; Summers, W. A.; Colon-Mercado, H. R.; Elvington, M. C.; Steimke, J. L.; Steeper, T. J.; Herman, D. T.; Gorensek, M. B., Recent advances in the development of the hybrid sulfur process for hydrogen production. *ACS Symp. Ser.,* **2009,** *238*.
11. Steimke, J. L.; Steeper, T. J.; Colon-Mercado, H. R.; Gorensek, M. B., Development and testing of a PEM SO2-depolarized electrolyzer and an operating method that prevents sulfur accumulation. *Int. J. Hydrogen Energy,* **2015,** *40*, 13281-13294.
12. Xue, L. L.; Zhang, P.; Chen, S. Z.; Wang, L. J., Pt-based bimetallic catalysts for SO2-depolarized electrolysis reaction in the hybrid sulfur process. *Int. J. Hydrogen Energy,* **2014,** *39*, 14196-14203.
13. Diaz-Abad, S.; Millan, M.; Rodrigo, M. A.; Lobato, J., Review of Anodic Catalysts for SO2 Depolarized Electrolysis for "Green Hydrogen" Production. *Catalysts,* **2019,** *9*.
14. O'Brien, J. A.; Hinkley, J. T.; Donne, S. W., Electrochemical Oxidation of Aqueous Sulfur Dioxide II. Comparative Studies on Platinum and Gold Electrodes. *J. Electrochem. Soc.,* **2012,** *159*, F585-F593.
15. Quijada, C.; Rodes, A.; Vazquez, J. L.; Perez, J. M.; Aldaz, A., Electrochemical-behavior of aqueous sulfur-dioxide at polycrystalline Pt electrodes in acidic medium - a voltammetric and in-situ FT-IR study .2. promoted oxidation of sulfur-dioxide - reduction of sulfur-dioxide. *J. Electroanal. Chem.,* **1995,** *398*, 105-115.
16. Rodriguez, J. A.; Liu, P.; Perez, M.; Liu, G.; Hrbek, J., Destruction of SO2 on An and Cu Nanoparticles Dispersed on MgO(100) and CeO2(111). *J. Phys. Chem. A,* **2010,** *114*, 3802-3810.
17. Quijada, C.; Vazquez, J., Electrochemical reactivity of aqueous sulphur dioxide at polycrystalline noble metal electrodes in acidic media. *Recent Res. Dev. Electrochem.,* **2000,** *3*, 137-181.
18. Zelinsky, A. G., Features of Sulfite Oxidation on Gold Anode. *Electrochimica Acta,* **2016,** *188*, 727-733.
19. Kriek, R. J.; Rossmeisl, J.; Siahrostami, S.; Bjorketun, M. E., H-2 production through electro-oxidation of SO2: identifying the fundamental limitations. *Phys. Chem. Chem. Phys.,* **2014,** *16*, 9572-9579.
20. Falch, A.; Lates, V.; Kriek, R. J., Combinatorial Plasma Sputtering of PtxPdy Thin Film Electrocatalysts for Aqueous SO2 Electro-oxidation. *Electrocatalysis,* **2015,** *6*, 322-330.
21. Colon-Mercado, H. R.; Hobbs, D. T., Catalyst evaluation for a sulfur dioxide-depolarized electrolyzer. *Electrochem. Commun.,* **2007,** *9*, 2649-2653.
22. Lu, P. W. T.; Ammon, R. L., Sulfur-dioxide depolarized electrolysis for hydrogen-production - development status. *Int. J. Hydrogen Energy,* **1982,** *7*, 563-575.
23. Lu, P. W. T.; Ammon, R. L., AN INVESTIGATION OF ELECTRODE MATERIALS FOR THE ANODIC-OXIDATION OF SULFUR-DIOXIDE IN CONCENTRATED SULFURIC-ACID. *J. Electrochem. Soc.,* **1980,** *127*, 2610-2616.
24. *CRC Handbook of Chemistry and Physics*. CRC press: 2014.
25. Markovic, N.; Gasteiger, H.; Ross, P. N., Kinetics of oxygen reduction on Pt(hkl) electrodes: Implications for the crystallite size effect with supported Pt electrocatalysts. *J. Electrochem. Soc.,* **1997,** *144*, 1591-1597.
26. Paulus, U. A.; Schmidt, T. J.; Gasteiger, H. A.; Behm, R. J., Oxygen reduction on a high-surface area Pt/Vulcan carbon catalyst: a thin-film rotating ring-disk electrode study. *J. Electroanal. Chem.,* **2001,** *495*, 134-145.

27. Elvington, M. C.; Colon-Mercado, H.; McCatty, S.; Stone, S. G.; Hobbs, D. T., Evaluation of proton-conducting membranes for use in a sulfur dioxide depolarized electrolyzer. *Journal of Power Sources, 195*, 2823-2829.